

Vibrational thresholds near critical average coordination in alloy network glasses

J. C. Phillips

AT&T Bell Laboratories, Murray Hill, New Jersey 07974

(Received 17 December 1984)

Experimental evidence for vibrational thresholds in network glasses recently predicted theoretically is discussed. A number of thresholds are observed, some of which are ascribed to phase separation and some of which may arise from intrinsic network mechanical properties. The glasses are binary and ternary chalcogenide alloys of Ge and Sn with S and Se, and the experiments are either acoustical or optical (infrared absorption and Raman scattering), with variable composition and external pressure. The first direct evidence for an electrical coherence length in a network glass is identified and analyzed.

I. INTRODUCTION

Substantial progress has been made recently in interpreting the results of microscopic experiments on network glasses^{1,2} and relating these results to the macroscopic glass-forming tendency.³ These developments rely on comparison of the average internal stress in the network, as generated by valence force fields, with the number of atomic degrees of freedom available to accommodate these stresses. Phillips's qualitative theory⁴ has been made more rigorous by Thorpe.⁵ According to Phillips, the glass-forming composition is optimized mechanically by equating the number of force-field constraints which are intact at $T=T_g$ (the glass transition temperature) with the number of atomic degrees of freedom. Thorpe showed that in the range of glass-forming compositions, the system should contain rigid and floppy regions, the latter being associated with soft vibrational modes stabilized only by broken or ineffective force-field constraints, such as van der Waals forces between chains.⁴

An independent approach to the mechanical properties of disordered networks based on numerical simulations of the elastic properties of percolative monatomic lattices⁶ shows threshold behavior similar to that found in critical phenomena. Except for very close to threshold, this behavior is well described by mean-field theory.⁷ In order to apply phase-transition models to glasses the usual percolation picture of charge flow along nearest-neighbor bonds must be generalized to vector percolation of atomic displacements as determined by a valence force field which includes angular bond-bending forces in addition to nearest-neighbor bond-stretching forces. When this is done the glass composition at the mean-field percolative threshold coincides with that predicted by Phillips's original constraint theory.⁸

In general, one would expect linear increases in the number of force-field constraints to produce linear increases in the elastic constants in glass alloys, providing the glass consists of a homogeneous network of the Zachariasen type. The mean-field model^{7,8} and numerical simulations^{6,9} show that, in addition to this linear variation beginning at or very near the mean-field threshold, an additional term of order $(x-x_c)^f$ is expected, with f of

order 2. Measurement of this effect, together with the composition dependence of the glass-forming tendency itself,³ would provide direct evidence for interpreting glass formation in terms of mechanical critical behavior in a system close to but not in configurational equilibrium.

The first experimental study of the compositional dependence of the elastic properties by Gilroy and Phillips¹⁰ used a resonator method which gave relative variations of sound velocity and acoustic attenuation as functions of temperature for several compositions x in $\text{Ge}_x\text{S}_{1-x}$ and $\text{Ge}_x\text{Se}_{1-x}$ glass alloys. This method did not permit comparison of the sound velocities in different samples. Too few samples were used to provide quantitative brackets on x_c , the critical composition, which should be 0.2 in these alloys. The theory, however, was confirmed in the following sense, which was not recognized by Gilroy and Phillips, but which is apparent now because of the development of percolation models.⁶⁻⁸ Strong peaks in the attenuation were observed near 90 K (30 K) in GeS_4 (Se and GeSe_4) samples (Fig. 1), which were absent for $x > 0.33$. According to the percolation model, for $x \leq 0.2$ floppy regions percolate. The temperatures of the peaks are in the vibrational range associated with $\nu_2(F_2)$ tetrahedral vibrational modes (110 and 80 cm^{-1} for GeS_2 and GeSe_2 , respectively).¹¹ While the agreement is only qualitative and the data are sparse, the general behavior observed in this pioneering study is promising and warrants further acoustic experiments, especially near $x=x_c=0.2$.

An additional feature of *acoustic* experiments (which is not present in more microscopic experiments such as Raman or Mössbauer scattering) is that the acoustic wavelengths of order 10^{-1} cm are very sensitive to low-frequency large-cluster rotational vibrations, such as are involved in glass solidification from the supercooled liquid. The very large peak in acoustic attenuation in $g\text{-GeS}_4$ observed near 90 K (see Fig. 1) may involve such large-cluster rotational vibrations. According to the mean-field model, when the network is slightly under constrained (corresponding to x slightly less than $x_c=0.2$ in a $\text{Ge}_x\text{S}_{1-x}$ glass alloy) cyclical ($\Omega^2=0$) vibrational modes are present whose number goes to zero at $x=x_c$. When fluctuation or cluster internal-surface (non-mean-field) ef-

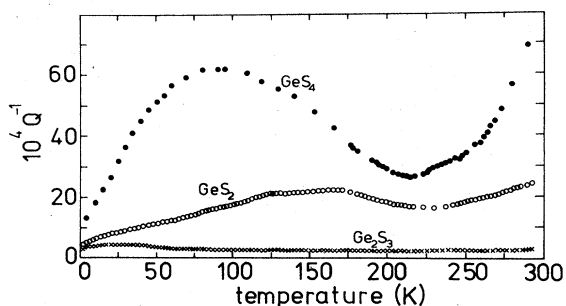


FIG. 1. Acoustic attenuation data (of K. S. Gilroy and W. A. Phillips) in several $\text{Ge}_x\text{S}_{1-x}$ glasses as a function of temperature, reproduced here from Ref. 10 for the reader's convenience.

fects are included, a small number of cyclical modes are present even at $x=x_c$. These modes tend to be much more delocalized¹² than the modes with $\omega^2 > 0$. Moreover, in the physical glass, weak intercluster van der Waals forces will be present which will shift cluster surface cyclical modes Ω and couple them to adjacent cluster surface modes. These are the modes which would couple most strongly to long-wavelength external acoustic waves. One can then understand why the attenuation in Fig. 1 is peaked so strongly near $T=90$ K. This corresponds to the F_2 -like cluster surface modes found in numerical simulations of GeS_2 -like cluster vibrations.^{12,13} Because of intercluster interactions the cyclical surface-mode frequencies Ω are shifted from $\Omega=0$ to just below the bulk or cluster interior F_2 GeS_2 frequency¹¹ of about 110 cm^{-1} . Starting from low T , large-cluster F_2 -like surface vibrations are first excited near $T=90$ K and these couple strongly to acoustic waves. At higher temperatures the cluster F_2 -like surface vibrations will be damped by coupling to F_2 -like cluster interior modes, and reduced acoustic wave attenuation will result. This model of soft F_2 -like cluster surface modes is consistent with recent Mössbauer studies of temperature-dependent cluster surface and interior Debye-Waller factors.¹⁴

The purpose of this paper is to draw attention to threshold behavior which has been observed by Raman scattering in certain *optic*-mode frequencies in chalcogenide glass alloys. Some of these thresholds appear at zero pressure as a function of composition. Although the percolation models stress *acoustic*-mode thresholds, it seems from the data discussed here that related thresholds may be present in data obtained on Raman-active optic modes. Additional thresholds, some of which may be of a nonpercolative nature, have been observed in high-pressure experiments on the same alloys. After reviewing the data^{15,16} for the reader's convenience, I discuss several theoretical models for the apparent threshold behavior.

II. RAMAN SCATTERING DATA

The effects of topological constraints on local vibrational frequencies can also be studied by augmenting the internal stress force field with external pressure. Murase and Fukunaga have made both Raman and infrared measurements at room temperature with a diamond-anvil cell on a wide range of $\text{Ge}_x\text{S}_{1-x}$ and $\text{Ge}_x\text{Se}_{1-x}$ binary alloys

and $(\text{Sn}_y\text{Ge}_{1-y})_x\text{Se}_{1-x}$ pseudobinary alloys.^{15,16} These pressure studies substantially extend the high-pressure experiments on $g\text{-GeS}_2$ carried out independently by Weinstein and Slade.¹⁷

In this paper I discuss some results of these studies theoretically. The discussion centers on the regime in which the number of constraints differs slightly from the number of degrees of freedom. In this regime the internal-strain energy generated by rigid and floppy clusters may both exhibit power-law dependences on $(x-x_c)$ for $y=0$ or $(y-y_c)$, where x_c and $y_c(x)$ are the topologically determined critical compositions. Because noncrystalline solids are not in equilibrium, these results cannot be exact. They are, however, valid to high accuracy because of the persistent metastability of network glasses, which results from their close proximity in free energy to equilibrium.

To achieve the precision needed to identify threshold compositions x_c^α and y_c^α and threshold pressures P_c^α (where α refers to a given partially polymerized cluster, such as a chain or a corner-sharing tetrahedron), as well as to determine power-law indices, high resolution is required. Such resolution has been achieved for selected narrow bands in the Raman spectra of the above-mentioned binary and pseudobinary alloys. Here I discuss results for (i) $\omega_{4\text{Ge}}^{A_1}(x)$ in $\text{Ge}_x\text{Se}_{1-x}$, corresponding to the A_1 symmetric breathing mode of corner-sharing $\text{Ge}(\text{Se}_{1/2})_4$ tetrahedra [$\omega_{4\text{Ge}}^{A_1}(\frac{1}{3})=202 \text{ cm}^{-1}$], (ii) the fraction of S_8 rings as measured by the integrated scattering strength I_8 of the alternating bending A_1 mode of S_8 rings ($\omega_{8u}^{A_1}=219 \text{ cm}^{-1}$) in $\text{Ge}_x\text{S}_{1-x}$ alloys, (iii) the pressure dependence of the A_1 stretching-mode frequency of S_n chains ($\omega_{nu}^{A_1}=475 \text{ cm}^{-1}$), as well as the A_1 tetrahedral modes of $\text{Ge}(\text{S}_{1/2})_4$ ($\omega_{4\text{Ge}}^{A_1}=345 \text{ cm}^{-1}$) and $\text{Sn}(\text{S}_{1/2})_4$ ($\omega_{4\text{Sn}}^{A_1}=316 \text{ cm}^{-1}$) in $\text{Ge}_{0.6}\text{Sn}_{0.4}\text{S}_3$ glass. Each of these clusters exhibits scaling behavior which I discuss in terms of its local rigidity and the global network constraints.

III. GLOBAL THRESHOLD BEHAVIOR

In Fig. 2 the compositional trends of several narrow Raman bands in $\text{Ge}_x\text{Se}_{1-x}$ glass alloys are shown for the reader's convenience as originally measured by Murase *et al.*¹⁵ Consider first the Se_n A_1 band associated with stretching modes of Se chains. As indicated in the figure, the broad behavior here is linear, indicating increasing internal stress as the average coordination number increases from 2.0 (at $x=0$) to 2.67 (at $x=0.33$). Some nonlinear behavior may be present near $x=0.2$. While more experimental points are needed to draw conclusions confidently, it appears that there is a discontinuity near $x=0.2$ corresponding to $\delta\omega \sim 3 \text{ cm}^{-1}$. The experimental uncertainty is $\Delta\omega \lesssim 1 \text{ cm}^{-1}$, and so this discontinuity may be significant. One possible explanation¹⁸ for the discontinuity is that for $x < 0.2$ the Se_n chains form $(\text{Se}_n)_m$ bundles of chains, whereas for $x > 0.2$ the Se_n chains are polymerized with outrigger GeSe_2 -like rafts. Thus, the Se is phase-separated for $x < 0.2$ on a scale of order 50 Å, but not for $x > 0.2$. This phase-separation threshold would be a consequence of the threshold percolation of rigidity at

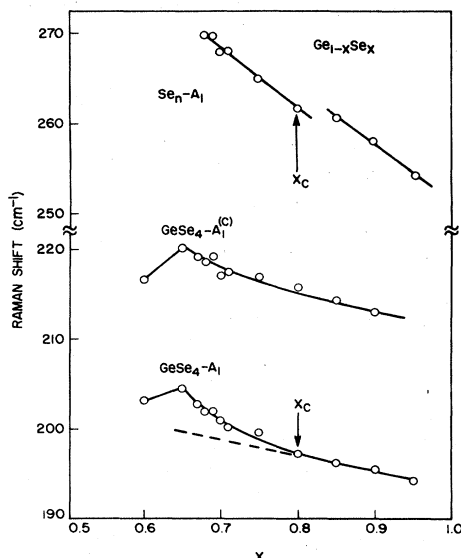


FIG. 2. Compositional dependence data (of K. Murase and collaborators) of tetrahedral (A_1 and $A_1^{(c)}$) and chain Se_n modes in Ge_xSe_{1-x} glasses, reproduced here from Refs. 15 and 16 for the reader's convenience.

$x=0.2$ and a corresponding threshold in the internal stress which disrupts the $(Se_n)_m$ -chain bundles.

More direct evidence is provided by the composition dependence of the A_1 and $A_1^{(c)}$ bands associated with the symmetric breathing modes of tetrahedra internal to and at the edges of "outrigger-raft" clusters.¹ The stress at raft edges due to reconstruction and intercluster interactions apparently obscures this threshold in $A_1^{(c)}(x)$, but it is quite apparent in $A_1(x)$; see Fig. 2. More accurate data are needed to establish the exponent f associated with this behavior, but $f=2.0\pm 0.5$ describes the present data adequately.

Let us consider next the effect of external pressure P_{ext} on the frequency $A_1(x, P_{ext})$ as reported recently by Murase and Fukunaga.¹⁶ This is shown in Fig. 3. At $x=x_c=0.2$ we might expect that application of pressure would effectively increase x because it increases A_1 . For $x=0.25 > x_c$, a first application of P_{ext} may have little effect because $P_{ext} < P_{int} \propto |x-x_c|$. Thus, we expect threshold behavior when $P_{ext} - P_{int}(x) > 0$. At $x=0.25$ it appears that this occurs near $P_{ext}=10$ kbar, while at $x=0.30$ the threshold seems to be at a larger value of P_{ext} (perhaps about 20 kbar, although data sparsity and scatter preclude quantitative analysis). The behavior shown in Fig. 3 suggests that application of external pressure to an overconstrained network at first compresses only the floppy regions, but then at a critical pressure (10 kbar for $x=0.25$) begins to convert floppy regions into rigid ones. This is a kind of pressure-induced phase mixing, for which more evidence is presented below.

IV. LOCAL THRESHOLD BEHAVIOR

In $g-Ge_xS_{1-x}$ glasses for $x \leq 0.2$, vibrational bands associated with the S_n chain at 475 cm^{-1} and S_8 rings at 475 and 219 cm^{-1} are observed. The composite character

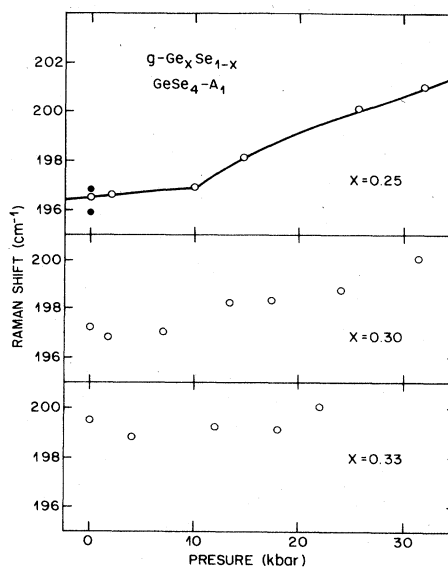


FIG. 3. Pressure dependence of A_1 modes, taken from K. Murase *et al.* (Ref. 16).

of the 475-cm^{-1} band renders analysis of threshold behavior difficult, but the 219-cm^{-1} band is narrow and isolated from other bands. Its integrated intensity¹⁶ is shown as a function of P_{ext} for $x=0.15$ and 0.20 in Fig. 4. The S_8 molecular population is extinguished near $P_e=22$ kbar for both compositions, although the volume filling at $P=0$ for $x=0.15$ is about twice as large as for $x=0.20$.

One can interpret common extinction pressures P_e , independent of x , as reflecting a structure in which the S_8 rings are embedded in S_n chains which, in turn, are embedded in GeS_2 -like clusters. The latter exert no direct pressure on the S_8 rings and hence P_e is independent of x , which modifies primarily only the internal pressure exerted by GeS_2 -like volumes on S_n regions. This example shows that local threshold behavior, not associated with percolating volumes, can exhibit intensive or "isolated-molecule" behavior.

V. TERNARY PHASE SEPARATION

The ternary glasses $Sn_yGe_{1-y}S_{2+n}$ and $Sn_yGe_{1-y}Se_{2+n}$, with $0 < n < 1$ and $0 \leq y \leq 0.6$, have at-

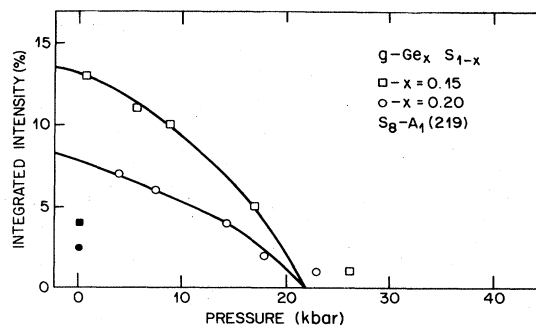


FIG. 4. Quenching of S_8 rings as a function of pressure in Ge_xS_{1-x} glasses, taken from K. Murase *et al.* (Ref. 16).

tracted much interest.² In this composition range almost all the Sn atoms enter the glass network substitutionally replacing Ge atoms. The Sn atoms are therefore tetrahedrally coordinated, as are the Ge atoms. However, at $T = T_g$, where the internal configurational stress is kinetically frozen, the contributions of Sn and Ge atoms to the internal stress field are quite different. This is because $T_m(\text{Sn}) \ll T_g \sim 800^\circ\text{C} \ll T_m(\text{Ge})$. Thus, each Ge atom contributes two bond-stretching and five bond-bending constraints to the network, while each Sn atom contributes only two bond-stretching constraints.¹⁹ Thus, although GeSe_2 (or GeS_2), which simply contains primarily tetrahedral building blocks, is overconstrained, the ternary is ideally constrained¹⁹ for y near 0.4.

We saw in Fig. 2 threshold behavior in the A_1 frequency in $\text{Ge}_x\text{Se}_{1-x}$ for $x=0.25$ slightly larger than $x_c=0.20$, but no microscopic explanation of the origin of the threshold was given. In Fig. 5 the Raman shifts of the tetrahedral $\text{Ge}(\text{S}_{1/2})_4$, $\text{Sn}(\text{S}_{1/2})_4$, and chain $\text{S}^n A_1$ modes under pressure, as measured by Murase and Fukunaga with a diamond anvil,¹⁶ are reproduced for the reader's convenience. Near 13 kbar something new and dramatic has occurred. For $0 < P < 13$ kbar the two tetrahedral A_1 frequencies increase *superlinearly*, but above 18 kbar both actually *soften*. The natural interpretation of this behavior is that above 13 kbar pressure fractures the network chemically, i.e., phase separation takes place. The solid circles in each figure describe the $P=0$ spectral peak positions after a compression cycle. Pressure-induced phase separation is inherently almost completely irreversible. Note that the $\text{Sn}(\text{S}_{1/2})_4 A_1$ peak frequency begins at 316 cm^{-1} , peaks near 322 cm^{-1} near 13 kbar, softens to 312 cm^{-1} at 30 kbar, and remains at

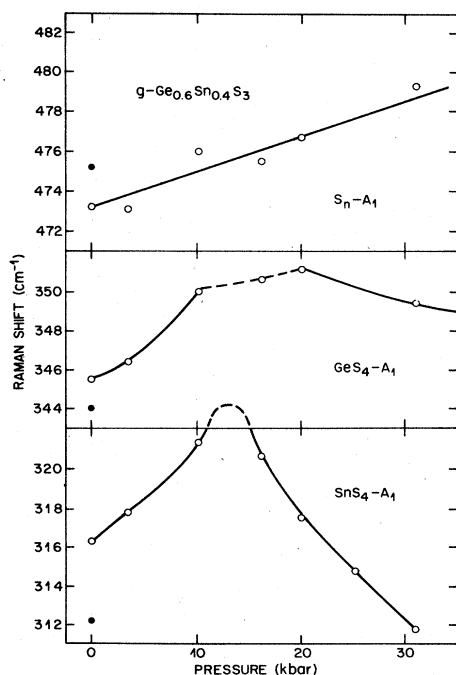


FIG. 5. Anomalous A_1 frequency shifts in ternary glass, taken from K. Murase *et al.* (Ref. 16).

312 cm^{-1} when P returns to 0.

Chemical fracture produces a strong threshold¹⁶ in the reduced bandwidth $\Delta\omega/\omega$, which is shown in Fig. 6. This threshold at 18 kbar is *common* to the $\text{Ge}(\text{S}_{1/2})_4$ and $\text{Sn}(\text{S}_{1/2})_4 A_1$ bands. This indicates that both tetrahedra belong to the *same* fractured network element. The existence of the threshold itself shows that this network element percolates through the glass.

VI. INFRARED SPECTRA

The infrared transverse- and longitudinal-optic (TO and LO) spectra of $\text{Ge}_x\text{Se}_{1-x}$ and $(\text{Sn}_y\text{Ge}_{1-y})_x\text{Se}_{1-x}$ glasses have been measured and discussed in excellent fashion by Murase and Fukunaga.¹⁶ While the scalar A_1 modes in these glasses are Raman active, it is the vector F_2 modes of the tetrahedral building blocks which are infrared active. For these modes we may also expect to observe threshold behavior, but the power laws should differ from those involved in scalar thresholds, although the threshold compositions should be the same. In the following discussion we recognize that the TO peak frequencies are peaks in $\omega\epsilon_2$, essentially absorption peaks, whereas the LO peak frequencies occur in $\omega \text{Im}(-1/\epsilon)$, where the complex dielectric function $\epsilon_1 + i\epsilon_2$ has been obtained by the Kramers-Kronig transformation.¹⁶

There are two F_2 peaks in the infrared spectra, a strong one near 260 cm^{-1} and a weak one near 310 cm^{-1} . The peak positions for the former are determined more accurately and it appears that there is a softening of the LO peak in $\text{Ge}_x\text{Se}_{1-x}$ glasses with a threshold at $x = x_c = 0.2$, as shown in Fig. 7. Although this interpretation may seem incomplete, we do notice that (1) the LO-TO splitting peaks near $x=0.25$, and (2) the LO peak position varies by 10 cm^{-1} while the TO peak position varies by $\leq 2 \text{ cm}^{-1}$. Because the LO mode involves long-range Coulomb interactions it is more sensitive to network stiff-

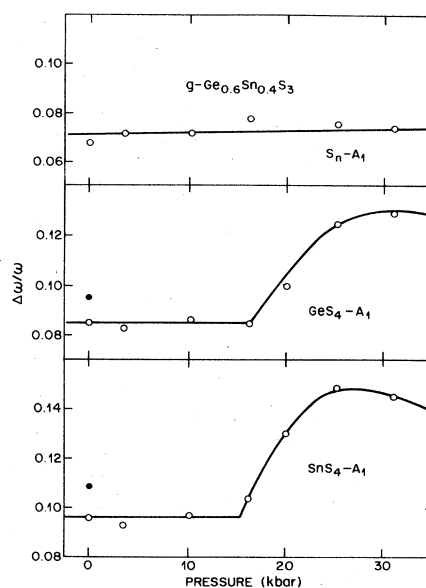


FIG. 6. Anomalous A_1 bandwidths in ternary glass, taken from K. Murase *et al.* (Ref. 16).

fening. Note also that in a naive continuous-random-network model of Ge^+Se^- dipoles, the density of the latter should increase linearly from $x=0$ up to $x=0.33$, and then decrease linearly as $\text{Ge}_2(\text{Se}_{1/2})_6$ ethane-like building blocks are formed up to $x=0.40$. This is clearly not the case for the data shown in Fig. 7. The linear increase includes a constant term (due to cluster formation) up to $x=0.2$, and above $x=0.2$, the LO peak softens approximately linearly. This suggests that mechanical stiffening of the network is reducing e^* , the dynamical effective charge responsible for the LO-TO splitting.

The data for the ternary glass alloys $(\text{Sn}_y\text{Ge}_{1-y})_{1-x}\text{Se}_x$ are very dramatic. They are shown in Figs. 8(a), 8(b), and 8(c) for $x=0.75$, 0.80, and 0.86, and they incorporate a new tetrahedral mode near 230 cm^{-1} associated with $\text{Sn}(\text{Se}_{1/2})_4$ units. The (TO,LO) pair associated with these tetrahedra generally shows zero splitting until a threshold value of $y=y_0(x)$ is reached. Above this threshold, as shown in Figs. 8(a)–8(c), the TO and LO modes split symmetrically (TO down, LO up) so that the average frequency remains nearly constant. (Note that this behavior is qualitatively different from that shown in Fig. 7, where the TO-mode frequency is nearly independent of composition.)

From the data shown in Figs. 8(a)–8(c) it is clear that the (TO,LO) F_2 modes of $\text{Sn}(\text{Se}_{1/2})_4$ tetrahedra are *not* split by Coulomb interactions with Ge^+Se^- dipoles, but instead are split only by resonant interactions with other Sn^+Se^- dipoles, which must vibrate in phase. Moreover, $y_0(x)$ has the remarkable form

$$y_0(x) = 4(x - x_c), \quad x > x_c \quad (1)$$

$$y_0(x) = 2(x_c - x), \quad x < x_c \quad (2)$$

where $x_c=0.20$. This is the same value of x_c used to analyze Fig. 7, and it is the value of x_c used to analyze the A_1 modes of $\text{Ge}_x\text{Se}_{1-x}$ glasses (Fig. 2) and predicted

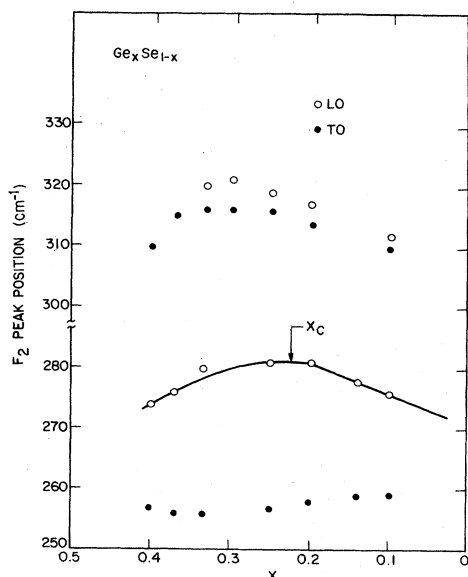


FIG. 7. Threshold behavior of LO-TO $\text{Ge}(\text{Se}_{1/2})_4$ splitting in binary $\text{Ge}_x\text{Se}_{1-x}$ glasses.

theoretically.⁴ Unless $x=x_c$, the Sn^+Se^- dipoles vibrate resonantly only above a concentration $y_c > 0$. However, the resonant vibrational range tends to infinity when x tends to x_c . This is a clear-cut characteristic of critical behavior.

It is perhaps surprising that the apparent range of Coulomb interaction responsible for the LO-TO splitting seems to decrease as $|x-x_c|$ increases. For $x=0.33$ critical behavior near $y=y_c=0.4$ has been inferred from the disappearance of internal surface states.^{2,19} However, for $y=0$ the internal surface states, as monitored by the presence of the $A_1^{(c)}$ Raman line, disappear near $x=0.12$ and are certainly present at $x=x_c=0.20$. Thus, the disappearance of cluster effects may be the signature of critical behavior near $x=0.33$, but they are not a necessary condition of critical behavior. A possible explanation for the behavior shown in Figs. 8(a)–8(c) is that near $x=x_c$ there is no screening of the $\text{Sn}(\text{Se}_{1/2})_4$ Coulomb interactions by the ideal $\text{Ge}(\text{Se}_{1/2})_4$ tetrahedral sea, but that with increasing $|x-x_c|$ screening develops from either F_2 -like latent cyclical modes (see discussion of Fig. 1) or from admixture of a dipole moment into acoustic modes by excess constraints.^{7,8} This explanation involves subtle features of the eigenvibrational modes of the network in the critical region. While elucidation of these subtle features is a formidable mathematical task which lies well outside the scope of this paper, I believe it is worth while to draw attention to a physical mechanism which is consistent with these remarkable data.

VII. DISCUSSION

Many examples of threshold behavior are illustrated in Figs. 2–8. Some of these are chemical but some may be mechanical, i.e., some are associated with phase separation but some may be ascribable to elastic percolation effects. Before making such an assignment, we note that at present elastic percolation models refer only to acoustic waves and specifically to anomalies in the velocity of sound.^{7,8}

If we suppose that the network is continuous, then various kinds of sum rules^{20,21} may apply to network vibrations of a given wavelength k . These sum rules could produce in the optic modes “echoes” of thresholds in acoustic modes.

The question of LO-TO splittings in glass networks has been discussed by Sekimoto and Matsubara using a phenomenological macroscopic theory.²² Their model is based on dipolar interactions between macroscopic sections of the glass. Payne and Inkson separate the internal electric field acting on each tetrahedron (in a tetrahedral glass such as $g\text{-SiO}_2$, $g\text{-GeSe}_2$, or $g\text{-Sn}_y\text{Ge}_{1-y}\text{Se}_2$) into two components, one of which is uniform and one of which is random.²³ It seems that according to the present analysis the uniform field is generally not in phase with the vibrations of an arbitrary tetrahedron. In the most favorable case [$x=x_c=0.2$ in $(\text{Sn}_y\text{Ge}_{1-y})_x\text{Se}_{1-x}$ glasses], the strength S_0 of the in-phase part of E_0 is proportional only to the density of identical tetrahedra. For the LO-TO splitting of the $\text{Sn}(\text{Se}_{1/2})_4$ tetrahedra, S_0 is proportional to y only. When $x \neq x_c$, S_0 is proportional to

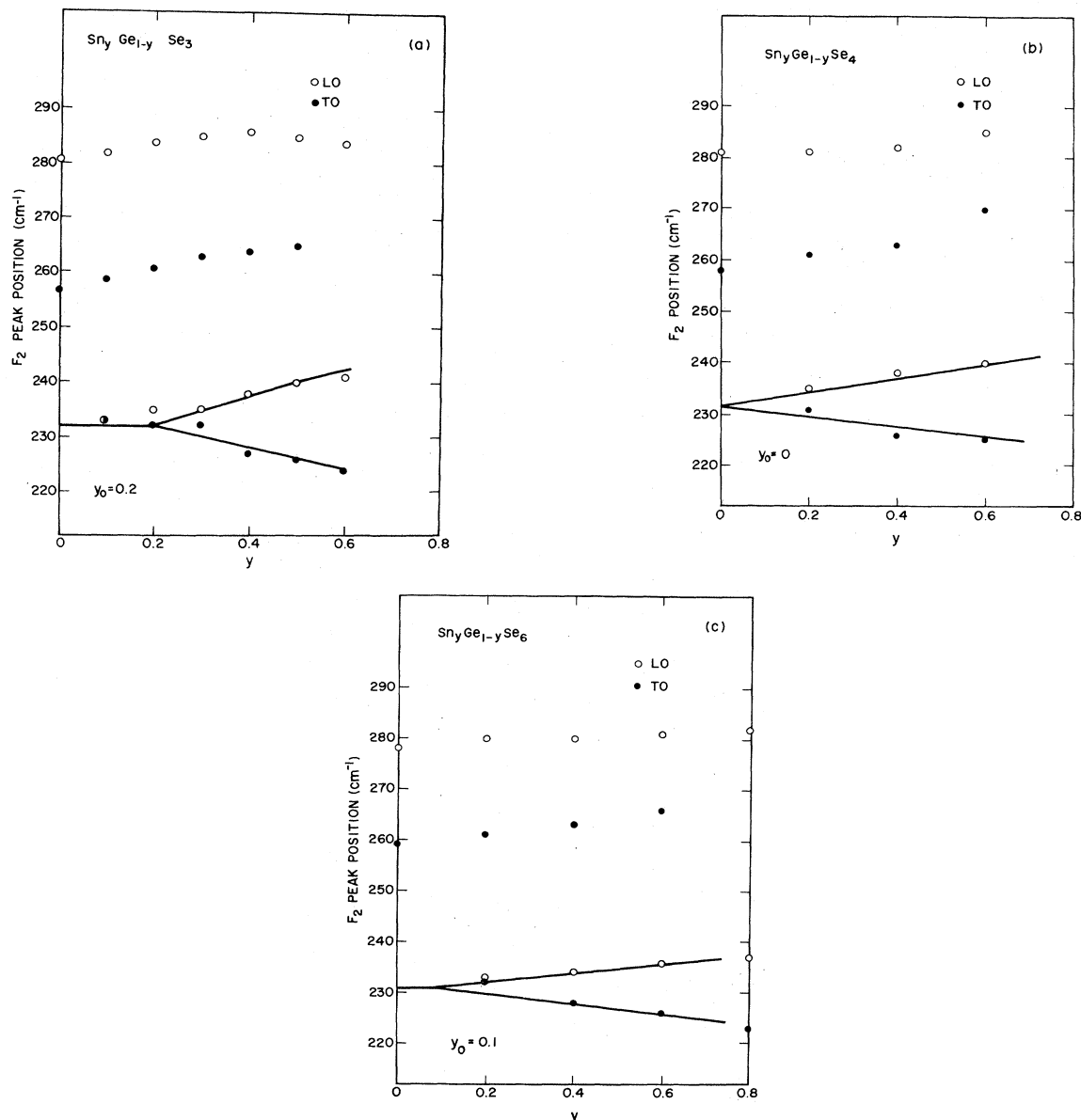


FIG. 8. Threshold behavior of LO-TO $\text{Sn}(\text{Se}_{1/2})_4$ splitting in ternary $(\text{Sn}_y\text{Ge}_{1-y})_x\text{Se}_{1-x}$ glasses. (a) $x=0.25$, (b) $x=0.20$, and (c) $x=0.167$.

$y - y_0(x)$ given by Eqs. (1) and (2) when this quantity is >0 ; otherwise S_0 is zero. This means that only tetrahedra within a range (or coherence length) $L \propto |x - x_c|^{-1/3}$ vibrate in phase with an effective local field. The separation made by Payne and Inkson should depend both on distance and on proximity of the glass composition to its ideal value. In a continuous-random network (composition unspecified) a self-consistent effective local electric field may be undefinable. However, the emergence of an observable coherence length of the internal electric field seems a natural consequence of topological and percolation models of network glasses.⁴⁻⁷

Many of the band shifts that have been illustrated for the A_1 tetrahedral modes are of order $5-10 \text{ cm}^{-1}$ compared to bandwidths (full width at half maximum) of order $10-20 \text{ cm}^{-1}$. At present the origin of the bandwidths

is not well established, but it has been suggested²⁴ that the bandwidth observed optically is a fraction f of the total bandwidth, where $f=d/D$ and d is a unit-cell diameter while D is a molecular cluster diameter. If D is a function of composition, then shifts in peak positions associated with bandwidth variations might be observed. However, except in the case of pressure-induced phase separation (Figs. 5 and 6), such shifts are not observed.

On the whole I favor, at present, mechanical stiffening as an explanation of threshold behavior, unless there is direct evidence for phase separation. The mechanical stiffening could affect explicitly cluster rotation, as discussed in the introductory section in connection with Fig. 1. However, further data are undoubtedly desirable to establish with confidence the microscopic origin of the thresholds discussed here. In this connection perhaps the most

generally valid remark which can be made is that so far threshold behavior generally occurs in the composition range predicted by my original constraint model.⁴

ACKNOWLEDGMENT

I am grateful to K. Murase and T. Fukunaga for stimulating correspondence and discussions.

- ¹J. E. Griffiths, G. P. Espinosa, J. C. Phillips, and J. P. Remeika, *Phys. Rev. B* **28**, 4444 (1983).
- ²M. Stevens, J. Grothaus, P. Boolchand, and J. G. Hernandez, *Solid State Commun.* **47**, 199 (1983).
- ³J. C. Phillips, *Physics Today*, **35**(2), 1 (1982); *Structure of Non-Crystalline Material*, edited by P. H. Gaskell, J. M. Parker, and E. A. Davis (Taylor and Francis, New York, 1982), p. 123; *Solid State Commun.* **47**, 203 (1983); G. H. Döhler, R. Dandoloff, and H. Bilz, *J. Non-Cryst. Solids* **42**, 87 (1980).
- ⁴J. C. Phillips, *J. Non-Cryst. Solids* **34**, 153 (1979); **43**, 37 (1981); *Phys. Status Solidi B* **101**, 473 (1980).
- ⁵M. F. Thorpe, *J. Non-Cryst. Solids* **57**, 355 (1983).
- ⁶S. Feng and P. N. Sen, *Phys. Rev. Lett.* **52**, 216 (1984).
- ⁷M. F. Thorpe, *J. Non-Cryst. Solids* **57**, 355 (1983); S. Feng, M. F. Thorpe, and E. Garboczi, *Phys. Rev. B* **31**, 276 (1985).
- ⁸J. C. Phillips and M. F. Thorpe, *Solid State Commun.* **53**, 699 (1985).
- ⁹H. He and M. F. Thorpe (unpublished).
- ¹⁰K. S. Gilroy and W. A. Phillips, *Philos. Mag. B* **47**, 655 (1983).
- ¹¹J. E. Griffiths, G. P. Espinosa, J. C. Phillips, and J. P. Remeika, *Phys. Rev. B* **28**, 4444 (1983).
- ¹²J. R. Banavar and J. C. Phillips, *Phys. Rev. B* **28**, 4716 (1983), and unpublished; J. A. Aronovitz, J. R. Banavar, M. A. Marcus, and J. C. Phillips, *Phys. Rev. B* **28**, 4454 (1983).
- ¹³K. Murase, T. Fukunaga, K. Yakushiji, T. Yoshimi, and I. Yunoki, *J. Non-Cryst. Solids* **59-60**, 883 (1983).
- ¹⁴P. Boolchand (private communication).
- ¹⁵K. Murase, T. Fukunaga, K. Yakushiji, T. Yoshimi, and I. Yunoki, *J. Non-Cryst. Solids* **59-60**, 883 (1983).
- ¹⁶K. Murase and T. Fukunaga, in Proceedings of the International Conference on the Physics of Semiconductors, 1984 (unpublished); in *Optical Effects in Amorphous Semiconductors, Snowbird, Utah*, edited by P. C. Taylor and S. G. Bishop (AIP, New York, 1984), p. 449.
- ¹⁷B. A. Weinstein and M. L. Slade, in *Optical Effects in Amorphous Semiconductors, Snowbird, Utah*, edited by P. C. Taylor and S. G. Bishop (AIP, New York, 1984), p. 457.
- ¹⁸J. C. Phillips, *Proc. Electrochem. Soc.* **82-9**, 147 (1982).
- ¹⁹J. C. Phillips, *Solid State Commun.* **47**, 203 (1983).
- ²⁰H. B. Rosenstock and G. Blanken, *Phys. Rev.* **145**, 546 (1966).
- ²¹R. M. Martin, *Phys. Rev.* **186**, 871 (1969).
- ²²K. Sekimoto and T. Matsubara, *Phys. Rev. B* **26**, 3411 (1982).
- ²³M. C. Payne and J. C. Inkson, *J. Non-Cryst. Solids* (to be published).
- ²⁴J. E. Griffiths, J. C. Phillips, G. P. Espinosa, J. P. Remeika, and P. M. Bridenbaugh, *Phys. Status Solidi B* **122**, K11 (1984).